6 Fabry–Perot Interferometer Filters

Ton Koonen

6.1 Operating Principles

6.1.1 Multi-beam Interference Process

A Fabry–Perot (FP) interferometer filter uses a multiple-beam interference process for obtaining wavelength selectivity. Usually, the filter has one input and one output port and employs two highly reflecting plates which together constitute the resonating cavity creating the multiple-beam interference process.

The basic concept of an FP filter is shown in Fig. 6.1. It was described first by Charles Fabry and Albert Perot in 1899 (Ann. Chim. Phys. Vol. 16). Two highly reflective planar plates are accurately positioned in parallel and thus form a cavity. A light beam entering the cavity is reflected multiple times between the plates. Each time when the beam hits a plate, a small part of its power escapes. When the two plates are aligned perfectly in parallel, the multiple beams escaping at each side of the FP cavity are exactly parallel. Each beam has a fixed phase difference with respect to the preceding one; this phase difference corresponds to the extra path length travelled in the cavity. The multiple parallel beams are brought into a common focus point with a lens, and in this point the actual multiple beam interference takes place. Hence, the amplitude of the transmitted electrical field E_t can be described by (see also [1])

$$\begin{aligned} E_t &= at^2E_i + at^2a^2r^2e^{-i\delta}E_i + at^2a^4r^4e^{-i\cdot 2\delta}E_i + \ldots \\ &\quad \ldots + at^2a^{2k}r^{2k}e^{-i\cdot k\delta}E_i \\ &= E_i \cdot t^2 \cdot a \cdot \sum_{k=0}^{\infty}\left(a^2r^2\right)^k e^{-i\cdot k\delta} = E_i \cdot \frac{a\cdot t^2}{1-a^2r^2\cdot e^{-i\delta}} \end{aligned} \tag{6.1}$$

where a is the amplitude attenuation factor when travelling once through the cavity, t is the amplitude transmission factor of a plate, r is its amplitude reflection factor.

Similarly, the amplitude of the reflected electrical field E_r is

$$\begin{aligned} E_r &= rE_i + t^2a^2re^{-i\delta'}E_i + t^2a^4r^3e^{-i\cdot 2\delta'}E_i + \ldots + t^2a^{2k}r^{2k-1}e^{-i\cdot k\delta'}E_i \\ &= E_i\cdot\left(r + \frac{t^2}{r}\sum_{k=1}^{\infty}\left(a^2r^2e^{-i\cdot\delta'}\right)^k\right) \\ &= E_i\cdot\left(r + \frac{t^2}{r}\cdot\frac{a^2r^2e^{-i\cdot\delta'}}{1-a^2r^2e^{-i\cdot\delta'}}\right) \end{aligned} \tag{6.2}$$

The phase shift δ (or δ') is the shift experienced between the directly transmitted (/reflected) beam and the beam which is transmitted (/reflected) after one roundtrip in the cavity.

With n being the refractive index of the medium between the plates, d the distance between the plates, θ the angle of incidence of the light, λ_0 its wavelength in vacuum, and ν is its frequency, the optical path length difference ΔS between the directly transmitted beam and the one transmitted after one cavity roundtrip is (see Fig. 6.2)

$$\Delta S = n\cdot(BC+CD) - BF = \frac{2nd}{\cos\theta'} - \sin\theta\cdot 2d\tan\theta' = \frac{2nd\,(1-\sin^2\theta')}{\cos\theta'} = 2nd\cos\theta' \tag{6.3}$$

where according to Snell's law $\sin\theta = n\sin\theta'$. The phase shift δ is therefore given by

$$\delta = \Delta S\cdot\frac{2\pi}{\lambda_0} = \frac{4\pi\cdot nd\nu}{c_0}\cdot\cos\theta' \tag{6.4}$$

Similarly, the optical path length difference $\Delta S'$ and the phase difference δ' between the directly reflected beam and the one reflected after one roundtrip in the cavity, taking into account an additional phase change of π when reflecting at an optically more dense medium, are

$$\begin{aligned} \Delta S' &= n\cdot(AB+BC) - AE = \frac{2nd}{\cos\theta'} - \sin\theta\cdot 2d\tan\theta' = 2nd\cos\theta' \\ \delta' &= \pi + \Delta S'\cdot\frac{2\pi}{\lambda_0} = \pi + \frac{4\pi\cdot n\,d\,\nu}{c_0}\cdot\cos\theta' \end{aligned} \tag{6.5}$$

The sharpest filter characteristics are obtained when all the multiple beams are collected by the lenses, so by operating as close as possible to normal incidence, i. e. $\theta \approx 0$.

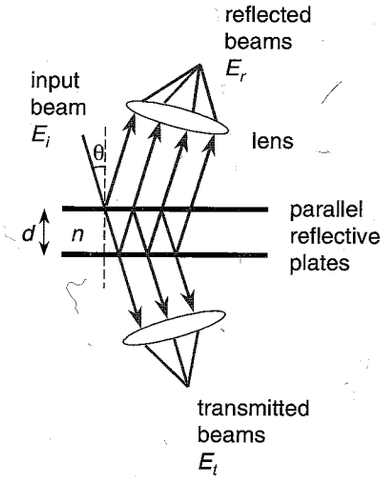

Fig. 6.1. Fabry–Perot Interferometer

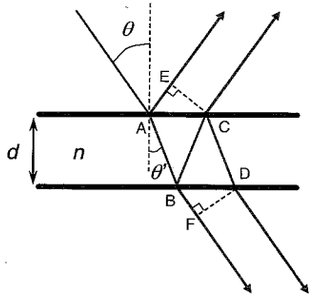

Fig. 6.2. Path length differences between transmitted and reflected beams

The intensity transmission factor T_{FP} of the Fabry–Perot filter, defined as the ratio of transmitted light intensity and the incident light intensity, follows the Airy function according to

$$T_{FP}(\nu) = \frac{I_t}{I_i} = \frac{E_t E_t^*}{E_i E_i^*} = \frac{T_0}{1+\left\{\frac{2}{\pi}F_R\sin\left(\frac{\delta}{2}\right)\right\}^2} \tag{6.6}$$

where the reflectivity finesse F_R and the maximum transmission factor T_0 are respectively

$$\begin{aligned} F_R &= \frac{\pi\sqrt{AR}}{1-AR} \\ T_0 &= \frac{AT^2}{(1-AR)^2} = \frac{A\,(1-R)^2}{(1-AR)^2} \end{aligned} \tag{6.7}$$

where $R=|r|^2$ is the intensity reflection coefficient of the plates, $T=|t|^2$ the intensity transmission coefficient, the plates are assumed to be loss free (so $R+T=1$), and $A=|a|^2$ is the attenuation factor of the light intensity when travelling from one plate to the other. The intensity transmission factor depends on the optical frequency ν through the dependence of the phase shift δ on ν.

Similarly, the intensity reflection factor R_{FP} of the Fabry–Perot filter, defined as the ratio of reflected light intensity and the incident light intensity, is

$$R_{FP}(\nu)=\frac{I_r}{I_i}=\frac{E_r E_r^*}{E_i E_i^*}=\frac{R_0+\left\{\frac{2}{\pi}F_R\sin\left(\frac{\delta}{2}\right)\right\}^2}{1+\left\{\frac{2}{\pi}F_R\sin\left(\frac{\delta}{2}\right)\right\}^2} \tag{6.8}$$

where the minimum reflection factor is

$$R_0=R\cdot\left(\frac{1-A}{1-AR}\right)^2 \tag{6.9}$$

If the medium between the plates is lossless (so $A=1$, which is a good approximation when air is used between the plates), then, as to be expected,

$$T_{FP}(\nu)+R_{FP}(\nu)=1 \tag{6.10}$$

6.1.2 Frequency Characteristics (Bandwidth, finesse, contrast ratio)

The dependence of $T_{FP}(\nu)$ on the optical frequency ν for a lossless FP is shown in Fig. 6.3. The characteristics $T_{FP}(\nu)$ and $R_{FP}(\nu)$ are periodic with a period called the Free Spectral Range FSR, given in the frequency domain by

$$FSR_\nu=\frac{c_0}{2nd}\quad[\text{Hz}] \tag{6.11}$$

and in the wavelength domain by

$$FSR_\lambda=\frac{\lambda_0^2}{2nd}\quad[\text{m}] \tag{6.12}$$

For example, when the plate distance $d=120\,\mu\text{m}$, $\lambda_0=1.55\,\mu\text{m}$, and $n=1$, $FSR_\lambda=10\,\text{nm}$.

Another useful performance parameter is the contrast factor C which is defined as the ratio of the maximum and the minimum of the intensity transmission factor $T_{FP}(\nu)$:

$$C=\frac{T_{FP,\max}}{T_{FP,\min}}=\left(\frac{1+AR}{1-AR}\right)^2 \tag{6.13}$$

This factor determines the crosstalk attenuation which is achievable when using the FP for selecting a wavelength channel out of a set of channels. For example, for a lossless medium between the FP plates (i. e. $A=1$) and a plate reflectivity $R=0.9$, $C=361$, which amounts to a crosstalk attenuation of 25.6 dB.

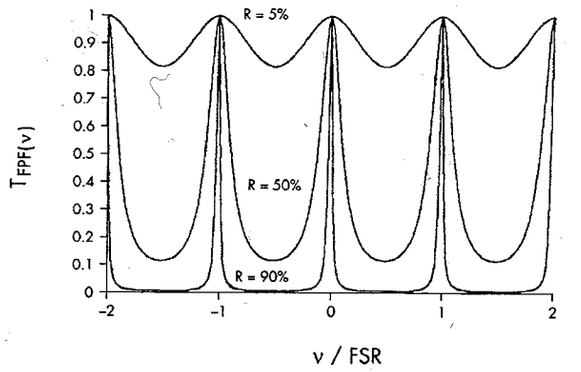

Fig. 6.3. Intensity transmission factor $T_{FP}(\nu)$ of a Fabry–Perot filter versus the light frequency ν normalized with repect to the free spectral range FSR (where R is the reflectivity of the plates)

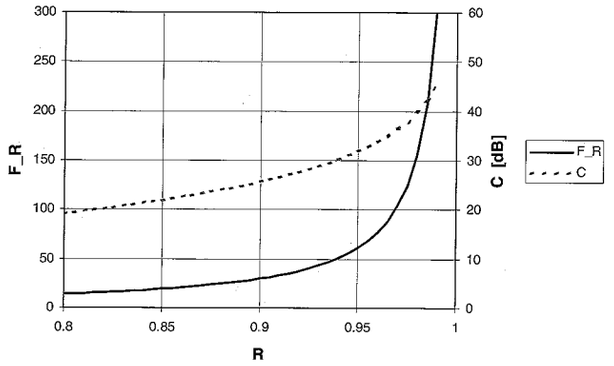

Fig. 6.4. Reflectivity finesse F_R and contrast factor C of a lossless Fabry–Perot filter versus the plate reflectivity R

The –3 dB bandwidth $\Delta\nu_{FWHM}$ (FWHM, full-width at half-maximum) of the FP bandpass curves $T_{FP}(\nu)$ is

$$\Delta\nu_{FWHM}=\frac{c_0}{2\pi nd}\cdot\frac{1-AR}{\sqrt{AR}}\quad[\text{Hz}] \tag{6.14}$$

and is related to the Free Spectral Range according to

$$\Delta\nu_{FWHM} = \frac{FSR_\nu}{F_R} \tag{6.15}$$

Hence, the ratio of the –3 dB bandwidth $\Delta\nu_{FWHM}$ and the FSR is only determined by the reflectivity R of the plates and the attenuation factor A of the medium between them.

6.2 FP Design Aspects

6.2.1 Instrument Finesse

The effective finesse of a Fabry–Perot filter may be lowered when the plates are not perfectly aligned: they may be not perfectly parallel, and/or not perfectly flat.

For instance, if the plates have a spherical curvature such that the distance between the plates measured in the centre and measured at the edges varies by λ_0 / M (where M is a positive real number), then the flatness finesse factor is to a good approximation given by [1]

$$F_F \approx M/2 \tag{6.16}$$

The resulting effective instrument finesse F_I of the FP is

$$F_I^{-2} = F_R^{-2} + F_F^{-2} \tag{6.17}$$

Commercial Fabry–Perot filters are available with instrument finesses from less than 30 to more than 200. The instrument finesse F_I is a measure of the resolution for wavelength filtering. In a multi-wavelength system, it e. g. determines the maximum number of wavelength channels which can be resolved. For instance, when a crosstalk attenuation of better than 10 dB is required (which implies a crosstalk power penalty of less than 0.5 dB), this maximum number of wavelength channels $N_{\max}$ is

$$N_{\max} \approx \frac{F}{3} \tag{6.18}$$

Hence an instrument finesse of $F = 100$ would allow to resolve up to some 30 wavelength channels.

6.2.2 Tuning

A Fabry–Perot filter may be tuned by changing the optical path length between the plates which can be done by changing the refractive index and/or the physical distance.

The refractive index may be changed for instance by changing the pressure of the gas (air) in the cavity; this will allow slow tuning only.

Changing the spacing between the plates can be done manually (by micrometer screws for coarse adjustment) and/or electro-mechanically. The fastest tuning is achieved with piezo-electrical transducers.

The maximum transmission is obtained when the optical path length matches an integer number times half the wavelength of the light in the cavity, so when

$$n\,d = m \cdot \lambda_0 / 2 \tag{6.19}$$

where m is an integer. Hence the transmission maxima occur at the optical resonance frequencies

$$\nu_{res} = \frac{c_0}{\lambda_0} = c_0 \frac{m}{2\,n\,d} \tag{6.20}$$

which are spaced by the Free Spectral Range $FSR_\nu = c_0 / 2\,nd$.

6.3 Practical Implementations

6.3.1 Free-space Bulk Fabry–Perot Filter

Planar etalon

In laboratory setups for high-resolution wavelength measurements with free-space optics, relatively large, modular planar FP etalons are used. The plate spacing is usually adjustable manually over a wide range which allows very high resolutions. Large diameter mirrors with high flatness (diameter up to ca. 2 inches, flatness $\lambda/200$ or even better) are commercially available, with broadband multilayer dielectric coatings achieving reflectivities over 98%.

As shown in Fig. 6.5, the setup consists of two lenses which collimate the light beam from the light source into a parallel beam which traverses the FP cavity, and subsequently through a pinhole focus the light on a detector. The cavity is composed of two mirror plates of which the facing sides are coated with a highly reflective coating; these sides are aligned in accurate parallelism. The plates are slightly wedge-shaped in order to prevent the outer sides to form a secondary FP cavity. When using a monochromatic source, a concentric Airy disc pattern appears in the focus plane of the second lens. On the Airy rings, the condition of constructive multiple beam interference is met. When the distance d between the plates is varied by means of e. g. piezo-electric transducers, the rings of the Airy

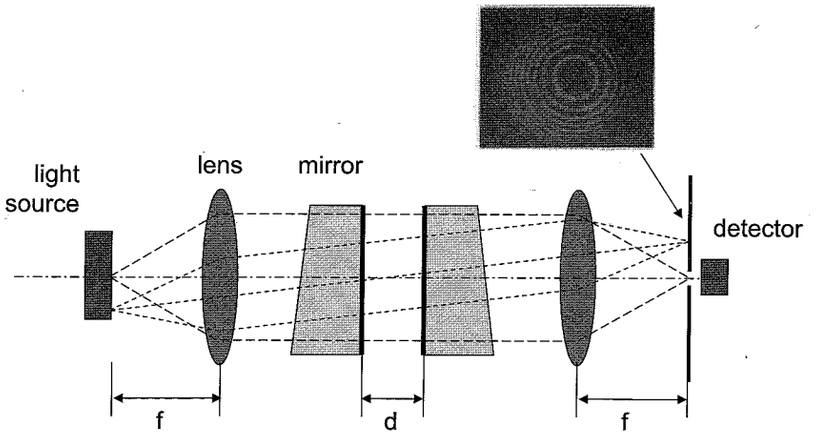

Fig. 6.5. Planar Fabry–Perot etalon

disc pattern are expanding or contracting. Through the pinhole, a detector is illuminated and will detect maximum signal when the cavity length d is an exact integer multiple of half the light source's wavelength (the resonance condition).

The FP mirror plates are mounted in a setup such as the one shown in Fig. 6.6. The distance between the plates can be set coarsely by sliding one of the mirror holders. The coarse adjustment of the mirrors to achieve parallelism is done with the three fine-threaded screws. One of the FP mirror plates is mounted on a piezo-electric transducer with three elements positioned under 120 degrees in order to enable both translation and tilting of the mirrors. The fine-tuning of the parallelism can be done by steering the elements individually in order to achieve the appropriate tilting. Sweeping of the plate distance is done by steering the three elements together. Putting

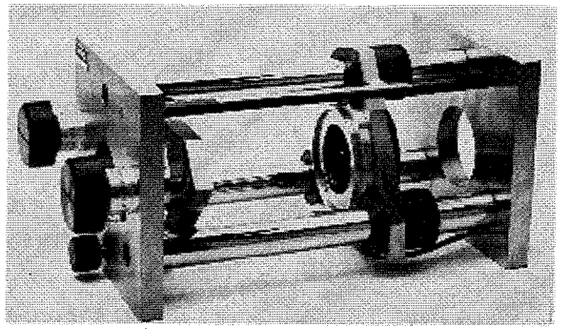

Fig. 6.6. Mounting setup for planar Fabry–Perot etalon [2]

ramp-shaped driving voltages on the piezo-s yields a linear sweep of the plate distance, and by applying the sweep voltage on the horizontal channel and the detector output on the vertical channel of an oscilloscope, the actual spectrum of the light source can be observed in nearly real time. The ramp slopes should be tuned to match the sensitivity of the piezo-electric transducers in order to maintain strict parallelism of the plates during scanning.

The planar FP etalon is very versatile, and the FSR can be changed over a wide range by changing the mirror separation. Mirror spacings may be set from a few μm up to more than 10 cm, yielding e. g. an $FSR_\nu = 1500$ GHz at $d = 100$ μm down to $FSR_\nu = 1.5$ GHz at $d = 10$ cm. However, the alignment of the mirrors needs careful tuning and is a delicate operation (asking extra caution when the mirror spacing is small, including careful removal of dust particles on the mirror surfaces). Instrument finesses typically can be around 150, yielding resolutions down to 10 MHz.

Confocal etalon

A confocal Fabry–Perot cavity uses two concave spherical mirrors which are separated by a distance equal to the radius of curvature of the mirrors [2]. As illustrated in Fig. 6.7, a complete roundtrip of a light beam through the cavity covers a path length of $L = 4 \cdot d = 4R$. The resonance condition $L = m \cdot \lambda_0 / n$ (with integer m) thus implies that transmission maxima occur at the optical frequencies

$$\nu_{res} = \frac{c_0}{\lambda_0} = m \cdot \frac{c_0}{4nR} \tag{6.21}$$

which are spaced by the Free Spectral Range $FSR_\nu = c_0 / 4nR$.

It is relatively easy to obtain a high finesse with a confocal FP interferometer because the narrow width of the incident beam reduces the finesse degradation due to mirror surface imperfections. Also the alignment procedure is simple as the mirrors just have to be positioned in a common

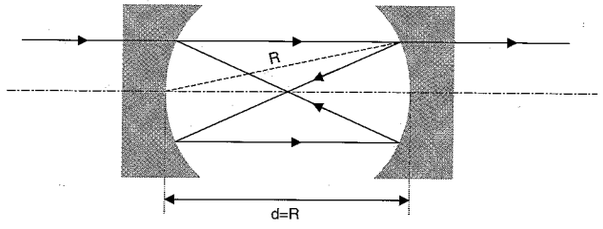

Fig. 6.7. Confocal Fabry–Perot interferometer

focus. However, the FSR is fixed by the mirror curvature radius; if the FSR needs to be changed, the mirrors must be replaced.

Commercial confocal etalons typically have FSR-s around 2 or 8 GHz, with instrument finesses from 200 to 300, yielding resolutions down to some 7 MHz. These etalons are well suited for detailed investigations of the spectra of narrowband lasers.

6.3.2 Fibre Fabry–Perot Filter

Fibre Fabry–Perot (FFP) filters fit readily into optical fibre communication links as they are equipped with single-mode fibre pigtails. No lenses or other collimating optics are used. The FP cavity is formed by two carefully aligned end faces of fibres on which a highly reflective coating has been deposited. Between the coated end faces the medium is air; in case of larger mirror spacings, a short piece of anti-reflection coated single-mode fibre may be inserted in the cavity which takes care of appropriate confined light guiding and of which the end face is anti-reflection coated in order to prevent secondary cavities. The basic structure of such a Fibre Fabry–Perot is shown in Fig. 6.8; a typical commercially available device is shown in Fig. 6.9 [3].

The spacing d between the highly reflective mirrors can be varied by means of piezo-electric transducers. Typically, maximum tuning voltages may be up to 70 V, and less than 12 V voltage swing is needed to traverse a Free Spectral Range. Depending on the coating design, the device may operate in the S-band (1480–1520 nm), the C-band (1520–1570 nm), the

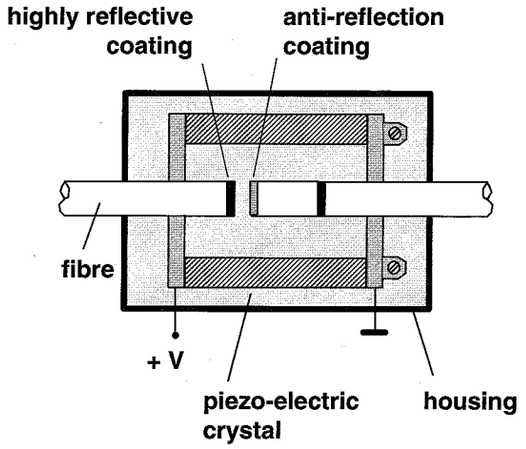

Fig. 6.8. Fibre Fabry–Perot filter

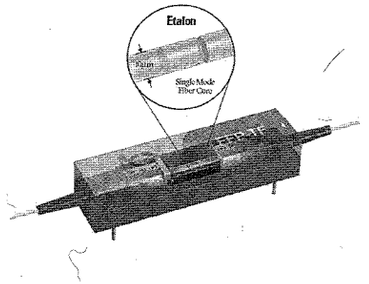

Fig. 6.9. Fibre Fabry–Perot module (courtesy of Micron Optics [3])

L-band (1520–1620 nm), or in the C- plus L-band. Instrument finesses may range from 10 up to 6000, and Free Spectral Ranges from 80 pm up to 250 nm (10 GHz to more than 31 THz). Due to the fibre-based design without extra optics, the fibre-to-fibre insertion losses are low (typically less than 2.5 dB). The circularly nearly symmetrical design makes the polarisation dependency low; typically less than 0.25 dB. The tuning speed is limited by the piezo-electric crystals; tuning over one FSR typically requires about 0.5 ms.

6.3.3 Gires–Tournois Filter

Similarly as a Fabry–Perot filter, a Gires–Tournois (GT) filter has a resonating cavity consisting of two parallel reflective plates. In a GT filter, however, one plate is fully reflective, whereas the other one is partly reflective. Hence, the GT interferometer can only work in the reflection mode, not in the transmission mode. The resonance condition is the same as with the FP, i. e. maximum reflection occurs when the plate spacing $d = m \cdot \lambda/2$, where m is an arbitrary integer. Equivalent to the Fabry–Perot, the Free Spectral Range is given by $FSR_\nu = c_0 / 2nd$. The GT's intensity reflection function basically has the same Airy function shape as the FP's one.

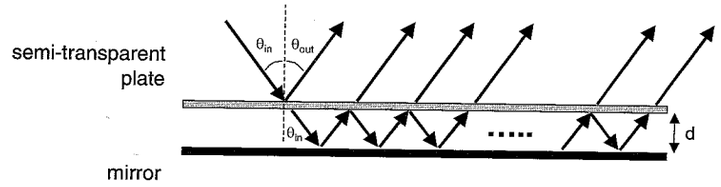

Fig. 6.10. Gires–Tournois interferometer

The Gires–Tournois filter is particularly suited for advanced spectral filter shaping, e. g. by inserting it in a Michelson interferometer setup, and by using e. g. micro-electromechanical systems (MEMS) – based micro-mirror arrays [4].

6.3.4 Interference Fabry–Perot Filter

A compact FP cavity can be realized by thin-film technologies. As shown in Fig. 6.11, a spacer region sandwiched between two reflecting layer stacks, deposited on a glass substrate, can constitute such an FP (see also [5]). The reflecting layer stacks usually are composed of $\lambda/4$-thickness layers, alternating of a high and a low refractive index. The reflection characteristics of these stacks become more square-top shaped with steeper edges when the number of layers is increased. Dielectric materials such as titanium dioxide ($n \approx 2.35$) and silicon dioxide ($n \approx 1.52$) are typically used in the 1.3–1.5 µm wavelength region. The dielectric spacer layer may be of high or low refractive index; the thickness of this layer is tuned such that the absolute frequency position and the Free Spectral Range requirements are met. The passband curves of the filter can be shifted to shorter wavelengths by tilting the incidence angle of the light. By this tilting, the phase shift δ between the transmitted beams would decrease when the wavelength is kept constant (see Sect. 6.1.1, equation (6.4)), and thus the wavelength needs to be reduced to get the same phase shift as with normal incidence, hence the filter curves shift to shorter wavelengths. However, the characteristics then also become dependent on the polarisation state; different curves shifted with respect to each other are experienced for TE- and TM-polarised light. This

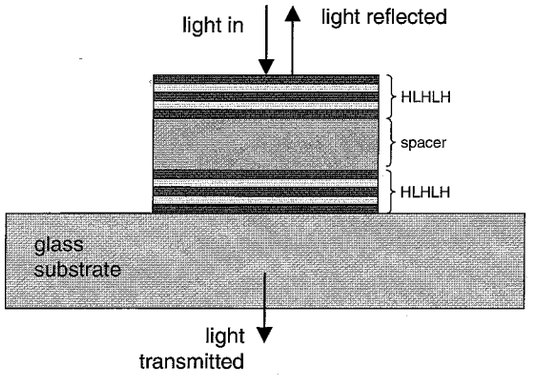

Fig. 6.11. Thin-fim Fabry–Perot interference filter

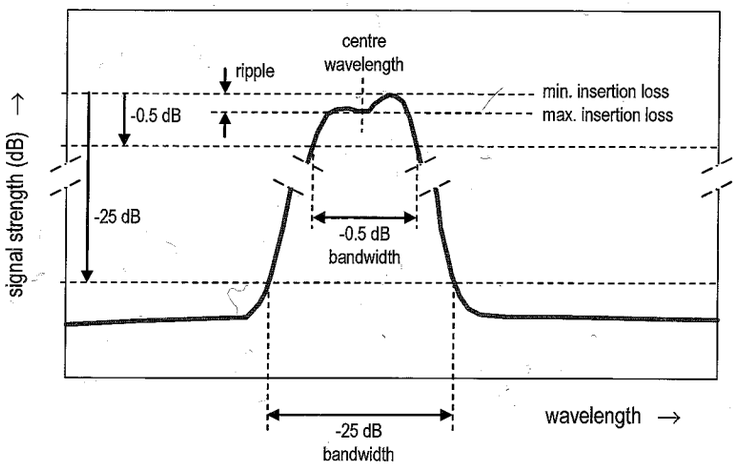

Fig. 6.12. Typical characteristics of a dielectric bandpass filter

polarisation-splitting deteriorates the filter performance for unpolarised light.

For smaller bandwidths, the peak transmission of the filter declines. DWDM dielectric bandpass filters are commercially available for wavelength channel selection according to the ITU grid (see e. g. [6]), having a –0.5 dB bandwidth of more than 0.7 nm and –25 dB bandwidth of less than 2.4 nm. The passband ripple can be less than 0.5 dB. The bandpass characteristics typically look as shown in Fig. 6.12.

6.4 Applications

6.4.1 Narrowband Single-channel Filtering

A tuneable Fibre Fabry–Perot can attractively be applied for channel selection in a multi-wavelength system, as illustrated in Fig. 6.13. The FSR should be larger than the range over which the wavelength channels are spread. Furthermore, the finesse should be high enough to resolve a single channel without too much crosstalk; as stated before, as a rule of thumb, the finesse should be at least three times the number of channels.

When an optical pre-amplifier is used (see Fig. 6.13), the tuneable FFP also cuts away the amplified spontaneous emission (ASE) noise spectrum which is not in the direct neighbourhood of the selected wavelength channel. This reduces the ASE-ASE beat noise and thus improves the receiver performance.

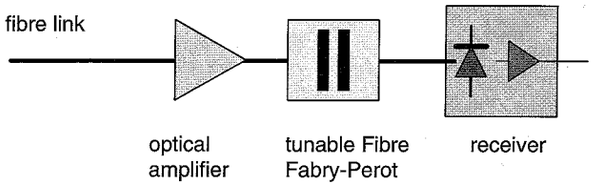

Fig. 6.13. Channel selection and pre-amplifier ASE filtering

The FFP can enable narrowband bandpass filtering, e. g. according to the ITU frequency grid definition for DWDM systems.

6.4.2 Optical Wavelength Channel Dropping

In multi-wavelength transmission networks, specific wavelength channels may be selected for dropping at intermediate nodes. For fixed-wavelength channel dropping, a Fibre Bragg Grating provides suitable characteristics. An FBG, however, is not easily tuneable over a wide wavelength range. A widely tuneable wavelength channel drop operation can be implemented with a tuneable FFP, as shown in Fig. 6.14 [9]. The FFP passes the selected wavelength channel λ_x for local dropping and reflects the other channels which then via the circulator and a coupler exit to the output fibre. At the coupler, another data signal at nominally the same wavelength λ'_x can be added. In its reflection path, the tuneable FFP needs to suppress adequately the selected wavelength channel and hence should have adequate notch-type characteristics (see also [3]).

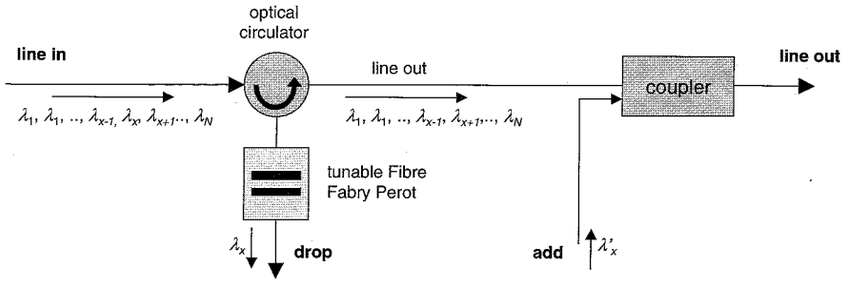

Fig. 6.14. Wavelength channel drop- and add-node, using a tuneable FFP

6.4.3 Multi-passband Filter

Multi-passband optical filters are useful in dense wavelength-division multiplexed transmission systems, e. g. when a number of wavelength channels need to be selected simultaneously from a noisy background (such as to cut ASE noise), or when a set of narrowly-spaced wavelength channels is to be split in two de-interleaved sets in order to ease channel processing. It is desirable to have flat-top square-shaped multi-passband characteristics in order to accommodate slight tolerances on the wavelength channel positions and to reduce any frequency-to-intensity modulation, such as may happen due to signal-induced chirp of the laser transmitters. These advanced multi-passband filter characteristics can be realized by e. g. including a Gires–Tournois interferometer in a Michelson interferometer, such as shown in Fig. 6.15. Such a filter can also be realized in all-fibre technology, as shown in Fig. 6.16, where the mirror function is implemented with a chirped Fibre Bragg Grating (FBG) and the Gires–Tournois filter with a composition of a weak fibre grating and a strong fibre grating, representing the beamsplitter and the mirror respectively in the GT architecture.

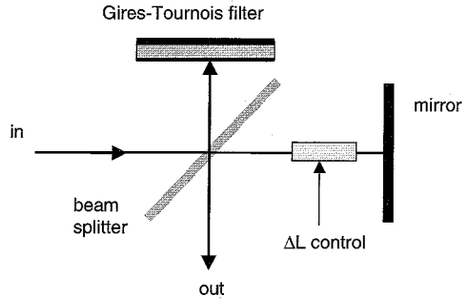

Fig. 6.15. Michelson–Gires–Tournois wavelength channel de-interleaver

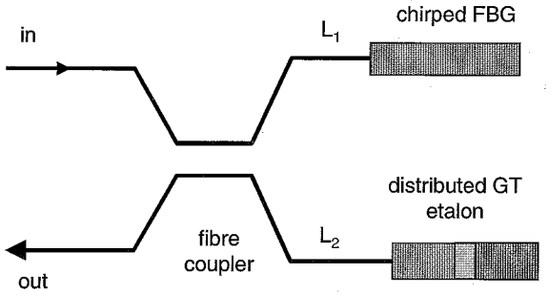

Fig. 6.16 All-fibre Michelson–Gires–Tournois filter

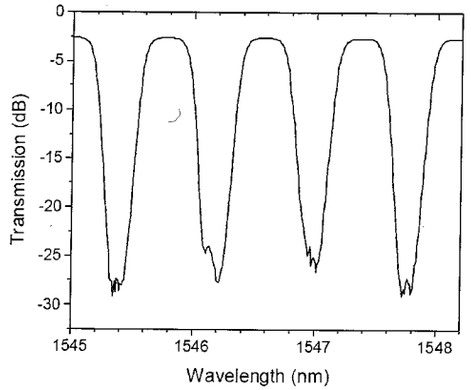

Fig. 6.17. Measured performance of all-fibre Michelson–Gires–Tournois filter

Measured spectra on this device show a nice wavelength de-interleaver performance (see Fig. 6.17) [7].

6.4.4 Wavelength Locking

In order to stabilize the wavelength of laser diodes which e. g. have to conform to the ITU frequency grid specifications of a high-density wavelength multiplexed system, Fabry–Perot filters can be applied in a so-called wavelength locker. The optical schematics are shown in Fig. 6.18 (see also [8]). Part of the output light of the laser to be stabilized is fed into the wavelength locker module where the total output power is monitored as well as the power at the desired wavelength position (to be set with the FP etalon). These two monitor output signals are then fed back to the laser transmitter unit for power- and wavelength-control. Commercially available wavelength lockers

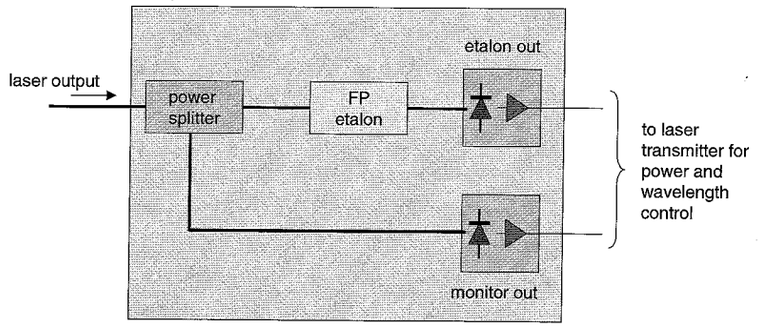

Fig. 6.18. Wavelength locker using a Fabry–Perot etalon

are designed for stabilization at 50 or 100 GHz wavelength channel spacing in the 1520–1620 nm range, conform the ITU grid. The centre channel accuracy can be within ±2.5 GHz; input powers up to 10 mW can typically be handled.

References

1. M. Born and E. Wolf: *Principles of Optics*, Chap. 7.6 (Pergamon Press, Oxford, 1980)
2. EXFO Burleigh, www.exfo.com
3. Micron Optics, www.micronoptics.com
4. O. Solgaard, D. Lee, K. Yu, U. Krishnamoorthy, K. Li, and J. P. Heritage: "Microoptical phased arrays for spatial and spectral switching," IEEE Commun. Mag. **41**, 96–102 (2003)
5. Melles Griot, www.mellesgriot.com
6. Edmund Optics, www.edmundoptics.com
7. X. Shu, K. Sugden, and I. Bennion: "Flattop multi-passband filter based on all-fiber Michelson-Gires-Tournois interferometer," *Proc. 30th Europ. Conf. Opt. Commun.* (ECOC'04), Stockholm, Sweden, 122–123 (2004), paper Tu1.3.1
8. JDS Uniphase, Broadband (Fabry-Perot) wavelength locker, www.jdsu.com
9. A. M. J. Koonen: "Multiwavelength Add/Drop Multiplexer," US Patent No. 5,751,456, issued on May 12, 1998